

Defect Tolerant High-temperature Superconducting Cable for the Central Solenoid of Compact Fusion Reactor

Vyacheslav Solovyov, Zachary Mendleson, and Makoto Takayasu

Abstract— The future compact fusion reactors, will feature very high, > 16 tesla, magnetic fields, which can be only created by magnet coils wound with the second generation (2G) superconducting wire. The 2G wires are currently manufactured with a thin (1-2 μm) YBCO layer deposited on a $\sim 100 \mu\text{m}$ thick metal substrate. The substrate makes up a considerable portion of the cross-section, thus reducing the engineering current density. It also prevents effective inter-filament current sharing, and the wide tape geometry is responsible for high magnetization loss. We report on the recent progress in the development of a new type of high-temperature superconducting cable architecture for the central solenoid of a high-field fusion reactor. The new architecture combines two recent innovations: (i) Reduction of AC loss by bundling narrow, 1-2 mm, exfoliated YBCO filaments into a cable, (ii) continuous winding and parallel slicing technologies, which eliminate labor-intensive and expensive handling of narrow filaments, critical for the central solenoid, which operates under pulsed load.

Index Terms— High-temperature superconductors, Superconducting cable, AC loss, fusion magnet

I. INTRODUCTION

The DEMO fusion reactor and the new generation of compact fusion reactors are proposed nuclear fusion power stations that are intended to build upon the ITER experiment. As with all fusion reactors based on plasma confinement, strong magnetic fields are essential to reduce the size and cost of the system and improve stability of the reactor. The DEMO reactor's central solenoid (CS) features magnetic fields reaching 18 T. To achieve resistive heating of the plasma, the field will be ramped within several seconds. At this time, the proposed CS cable design is a hybrid NbTi-Nb3Sn magnet with a high-temperature superconductor (HTS) insert [1], which utilizes the excellent current retention of HTS materials in a strong field.

HTS materials are considered for the new compact reactors (CR), Toroidal Field (TF) and CS coils [2]. The TF coils are expected to generate strong magnetic fields in the plasma volume, on the order of 9.5 T compared with the 5.7 T field of ITER. 2G HTS materials are the only known superconductors capable of supporting the much higher (23 T) on coil field of these new reactors. The progress in performance of second

generation (2G) high-temperature superconducting (HTS) wires enabled demonstration of ultra-high field, 26 T [3], [4]; more recently 40 T hybrid HTS magnets are being developed [5]. However, high AC loss, poor quench stability, and high cable cost prevents wider penetration of 2G wire technology into the magnet markets.

Magnetization loss is an important consideration in fusion energy systems. Consider, for example, the ITER TF. It is projected to have a total cryogenic heat load of 47 MJ per cycle. The conductor losses, both hysteresis and eddy-current, account for 24 MJ of loss, or 51%. We note that the ITER design uses a filamentized cable [3] with Nb3Sn strands measuring from 0.73 mm to 0.83 mm in diameter [6]. If instead, the much wider 4 - 12 mm 2G HTS tape were used, the loss would be increased by a factor of 6-10, thus imposing an impractically high load on the cryogenic plant. The AC loss contribution is even more critical for a small TF coil in a CR. Taking the coil ramp-up time to be 1 hour, the magnetization loss during ramp up would be on the order of 10 kJ. The AC loss would be proportionally higher for the DEMO reactor because of the high field. There are several approaches being developed for slicing 2G tapes into narrow filaments. However, it is impractical to handle and spool filaments narrower than 2 mm.

Magnets made from commercial 2G tapes are difficult to quench protect due to slow (1 cm/s) normal zone propagation and critical current anisotropy [7]. The quench protection and detection become even more problematic if a multilayer cable is made using conventional 2G tape. Narrow 2G filaments have limited lateral current sharing path's and poor vertical current sharing with adjacent layers. Thus, a quench in one filament may remain undetectable.

Here we describe a process for parallel slicing and cabling of a 1 mm wide twisted stack strand. A human operator handles only wide tape, >10mm. The tape is sliced, bundled, and twisted in one pass. Thus, eliminating the need for individual filament loading, spooling, and priming. We use exfoliated YBCO tape which allows for vertical current sharing within the filament stack thus significantly improving defect tolerance of the cable.

Manuscript received October 30, 2018; accepted February 19, 2019. Date of publication February 22, 2019; date of current version March 21, 2019. This work was supported by Supported by U.S. DOE Office of Science awards DE-SC0018737 and DE-SC0020832. (Corresponding author: Vyacheslav Solovyov.)

V. F. Solovyov is with Brookhaven Technology Group, 1000 Innovation Road, Stony Brook, NY 11794, (slowa@brookhaventech.com).

Zachary Mendleson is with Brookhaven Technology Group, 1000 Innovation Road, Stony Brook, NY 11794

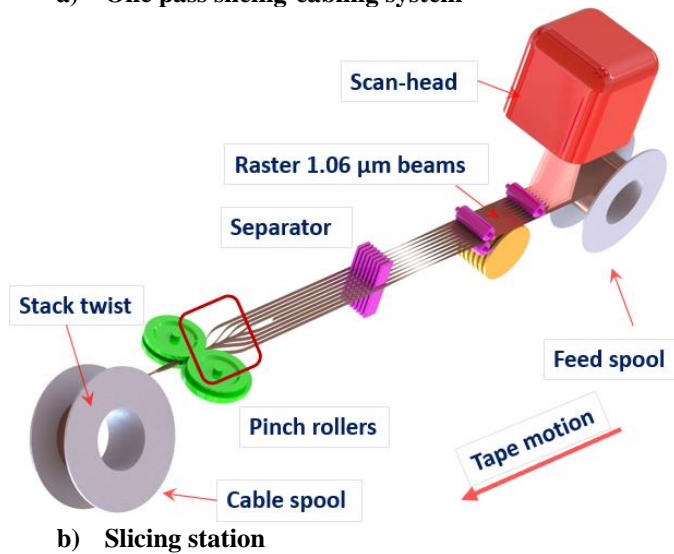
Makoto Takayasu is with the Massachusetts Institute of Technology, Cambridge, MA 02139 (e-mail: takayasu@psfc.mit.edu)

Color versions of one or more of the figures in this paper are available online at <http://ieeexplore.ieee.org>.
Digital Object Identifier

II. EXPERIMENT

We used a 10 mm wide exfoliated tape, comprised of a 1.2 μm thick YBCO layer attached to a 75 μm thick copper foil [8]. The main purpose of the exfoliation step was to eliminate the insulating substrate. The tape was coated with $10 \pm 2 \mu\text{m}$ of Sn-Pb solder in a custom coating system. The air-leveling was used to control the solder layer thickness. Fig. 1a is a schematic rendering of the cabling system. The tape is sliced into an array of filaments by a fiber laser (SPI 70w model) equipped with a scanning mirror system (IntelliScan 14 scan-head). The laser system projected a pattern of 10 lines, which was repeated by a computer command. The scanning pattern was synchronized with the tape motion so that a continuous cut was formed by

a) One pass slicing-cabling system



b) Slicing station

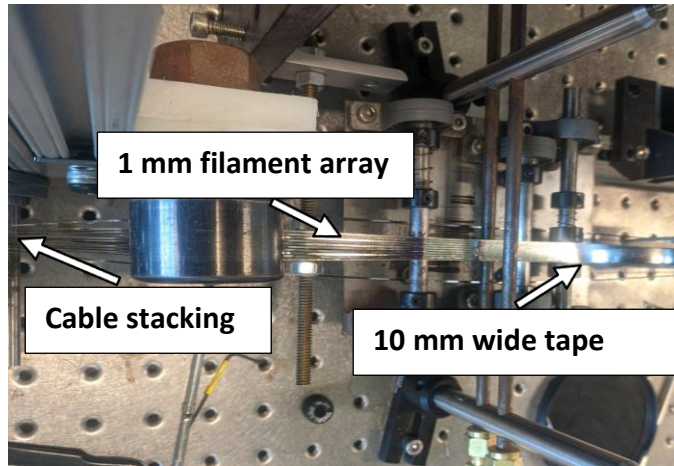


Fig. 1. a) Conceptual rendering of the parallel cabling system. b) Photograph of the slicing station of the cabling system. The laser beam is coming from top. An array of 1 mm filaments is well visible.

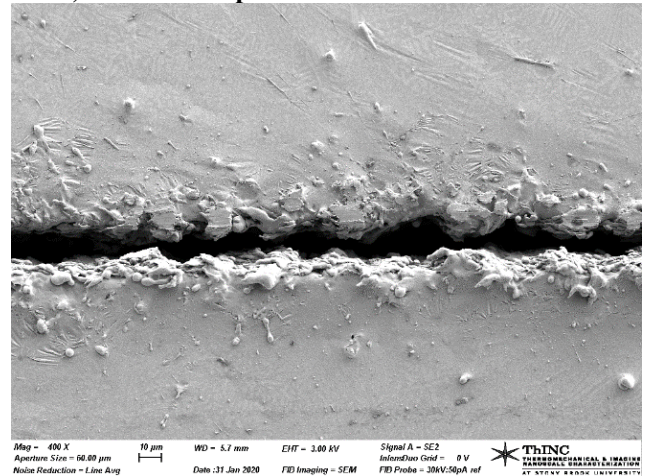
overlapping individual linear cuts. Fig. 1b is a photograph of the tape positioning setup, showing the 10 mm wide tape and the array of 10, 1 mm wide filaments.

The filament stack is further secured by pinch rollers and twisted. After twisting the cable is rapidly heated to 200°C to partially melt the solder and connect the filaments.

III. RESULTS

Fig. 2 presents results of the laser power optimization at the tape advance speed of 10 cm/s. The optimum power, 40 W in this case, produced a clean cut approximately 10 μm wide. A more powerful laser beam tends to eject large amounts of material on

a) 40 W laser power



b) 60 W laser power

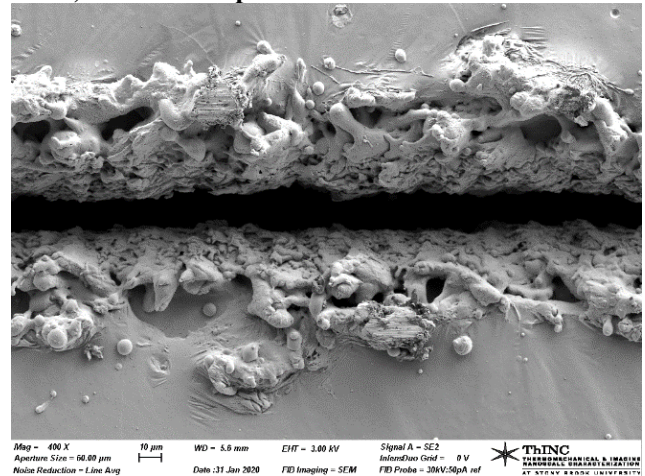
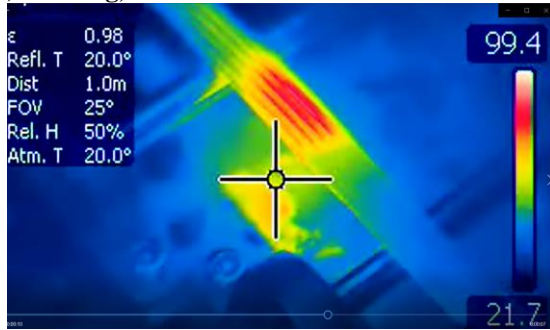


Fig. 2. Scanning electron microscope images of YBCO tape sliced at 40 W laser power, panel a) and 660 W laser power, panel b).

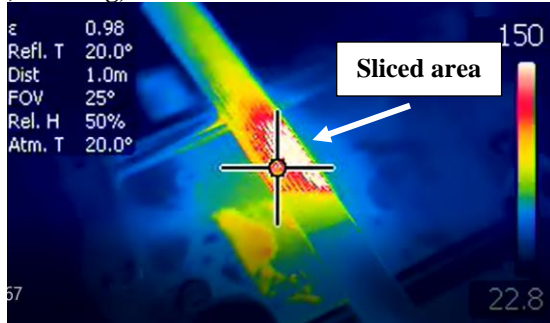
the tape surface, thus producing 50 μm wide damage zone, Fig 2b.

Nano-second laser pulses ablate the material, and most of the energy is consumed by vaporization and not by melting. Nevertheless, the heat load by the laser beam cannot be discounted. Fig.3 a and b compare infrared images of 10 mm wide tapes sliced in 2 mm filaments (panel a) and 1 mm filaments (panel b). Denser cuts in the case of 1 mm slices deposit larger amount of thermal energy which translates into higher tape temperature

a) Slicing, 2 mm filaments



b) Slicing, 1 mm filaments



c) Sliced filament arrays



d) Critical currents of filament arrays

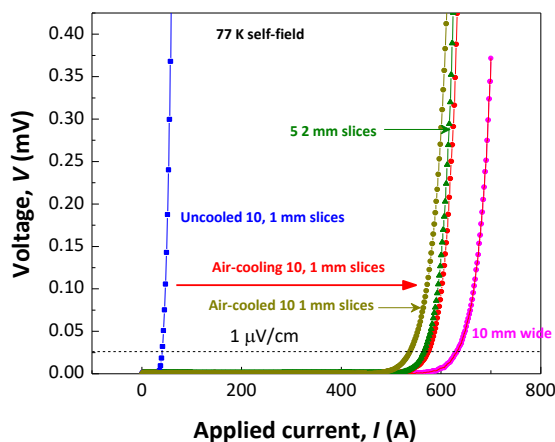


Fig. 3. a) Infrared image of 10 mm tape being sliced into 2 mm filaments. b) Infrared image of a 1 mm filament array, showing a significant temperature rise in the cut area. c) Critical current of the original 10 mm wide tape, and the same tape after slicing into 5, 2-mm and 1-mm filaments. The 1 mm wide filament required air cooling to retain the critical current above 90% of the original. d) I-V curves of the original tape and sliced filament arrays shown in panel c).

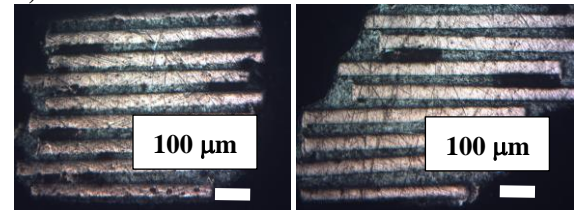
in the cut area. Overheating of the tape by laser beam is responsible for degraded performance of 1 mm filaments. Fig. 3d compares critical currents of arrays of 5 for 2 and 1 mm wide filaments (2, 5 and 10 filaments, correspondingly) to that of the original 10 mm wide tape. The actual filament arrays are shown in Fig 3c. The 10 mm wide tape, 20 cm long, is sliced in the middle with the fiber laser. The current is injected through the uncut end of the sample, which allows for a reliable evaluation of the slicing effect on the tape performance.

The I - V curve of a 10-filament array with 1 mm wide slices in the uncooled mode degraded well below 20 A. However, critical current of 2 mm and 5 mm array retained 90%

a) 1 mm cable



b) Cross-section



c) Critical current of a cable, 77 K

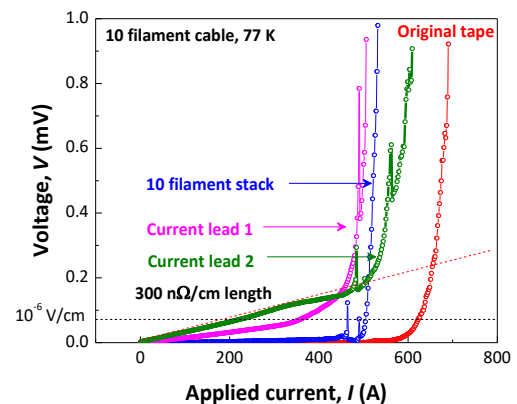


Fig. 4. a) Photograph of 1 mm wide filament comprised of a twisted stack of 10 exfoliated YBCO filaments. b) Cross section of the 1 mm wide filament, the “flat” section on the left and “twisted” area on the right. The right micrograph shows significant filaments sliding in the “twist” area. c) Critical current of the 1 mm cable compared to the original 10 mm wide tape. I - V curves of the current leads demonstrate that > 300 n Ω /cm lead electric resistance can be achieved by soldering the cable without the need for separating the cable into individual filaments. The dashed line is the linear fit of the resistive part of the I - V curve, corresponding to 300 n Ω /cm resistivity.

of the original current. A simple analysis shows that a small amount of thermal energy, approximately 20 W needs to be lifted from the tape surface to maintain the

overall temperature below 100°C. A moderate air flow, 1.5 L/s is sufficient in evacuating this level of heat from the tape surface. Indeed, introduction of air cooling restores the critical current to the level above 90% of the original, see Fig. 3d.

Fig. 4b is a photograph of the 1 mm wide twisted stack cable. The stack is comprised of 10, 1 mm wide, 60mm pitch twisted filaments. After the twisting step the stack is fused by melting the solder coating. Fig. 4b shows a cross-section of the cable in the “flat” area, that is the area where the cable lies flat on the mandrel and the transitional region between two opposing cable orientations. In the “flat” area the filaments are stacked vertically, while in the “twisted” region the filaments noticeably sliding against each other. Unimpeded sliding of the filaments during twisting is important for avoiding damage to the YBCO layer. This type of cable can be fused only after the twisting step.

Fig. 4c compares I - V curves of a 20 cm cable coupon compared with the original 10 mm wide tape. We also present I - V curves of the current leads, which were made by direct soldering of the cable to the copper block, without separation of the cable into individual filaments. We assign approximately 20% loss of I_c to the filament edge damage due to the filament edge overheating. The experiment also demonstrates that current leads with resistivity ≈ 300 n Ω /cm can be made by soldering to the cable. In comparison, typical contact resistivity of 10 mm wide tape (YBCO to YBCO) is ≈ 100 n Ω /cm. Finally, Fig.5 demonstrates defect-tolerance of the cable. Here 5 filaments were stacked and fused, while one filament was intentionally cut. The overall critical current density is reduced 15 A, that is half of the reduction that would occur if the filaments were uncoupled.

IV. DISCUSSION

Cabling YBCO conductors is challenging because the ceramic YBCO layer can only sustain elastic deformation $<0.5\%$ of in-plane strain. The somewhat better tolerance of YBCO to compressive strain allows the design of spiral wound, so-called CORC cables [9]. However, realizing a strand with a cross section < 1 mm x 1 mm is essential in avoiding large magnetization loss in a magnet, which is difficult to accomplish by spiral winding. Laser slicing offers a way to slice filaments < 1 mm width and the twisted stack is arguably the simplest cable design that fully utilizes such filaments [10]. In our prior work we have shown that a continuous wave laser, such as CO₂, deposit high amount of heat into the cut area which needs to be evacuated by high flow of assisting gas [11]. The assist gas flow can easily shift the tape resulting in an uneven cut. A pulsed laser coupled with a fast scanning mirror can slice a 10 mm tape into 1 mm filaments at a moderate heat load in a reel-to-reel mode. However, air cooling is still required to keep the tape temperature below 100°C, Fig.3b.

The stacking and cabling steps need to immediately follow slicing. The sliced filament arrays, such as shown in Fig 3c cannot be spooled and subsequently cabled. This is because after the tape is sliced, a small amount of strain, which is always present, is released, resulting in a slightly different elongation of filaments. This effect prevents uniform tensioning of filaments and

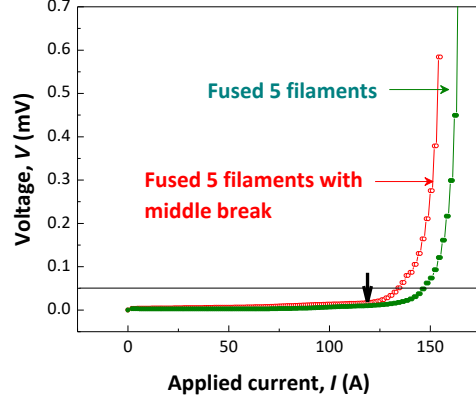


Fig. 5. Critical current of a 5 filament stack, one filament is cut on purpose. The vertical arrow shows critical current of a 4 filament cable. The experiment demonstrates defect-tolerance of the cable design.

spooling of the arrays without crossing or twisting of the filaments. The effect is alleviated in a twisted stack, where slight variations of the filament elongation are cancelled by the partial transposition. An alternative would be spooling of individual 1 mm wide filaments and applying individual tension to every filament. This is possible in theory, but is probably impractical, at least on the production scale.

Defect tolerance has gained a lot of attention recently when it became clear that defects in YBCO layer are unavoidable. Moreover, some defects remain undetected by off-line quality control methods and reveal themselves only after a coil is energized. Levin et al. [12] estimate that even a hairline fracture in the YBCO layer of a 4 mm wide conductor would have equivalent resistance as high as 7.5 $\mu\Omega$. So-called no-insulation magnet technology [13], [14] offers a solution at the expense of very large ramping loss and poor field quality. This cable architecture enables defect tolerance by allowing current to flow freely between the filaments at an expense of 10% critical current reduction, see Fig. 5. A magnet manufactured from the cable would still benefit from current sharing but unlike a no-insulation magnet, would be able to sustain much faster ramping. Finally, we note that the cabling process demonstrated in this work does not address tolerance to large defects that cross the whole 10 mm wide filament, such as a long crack. Because the filaments are coming from the same tape, a cross-tape defect would block current across the cable in one location leaving no possibility for current re-distribution. To eliminate sensitivity to such a defect, filaments must be coming from different tape coupons.

V. CONCLUSION

In conclusion we demonstrate a feasibility of manufacturing a narrow, 1 mm x 1 mm (1.5 mm diameter) cable that used a parallel slicing-cabling process. The cable is intrinsically defect tolerant due to utilization of exfoliated filaments that allow for easy current transfer between the filaments.

REFERENCES

- [1] R. Wesche, N. Bykovsky, X. Sarasola, K. Sedlak, B. Stepanov, D. Uglietti, and P. Bruzzone, "Central solenoid winding pack design for DEMO," *Fusion Engineering and Design*, vol. 124, no. 2017/11/01/2017, pp. 82-85.
- [2] B. N. Sorbom, J. Ball, T. R. Palmer, F. J. Mangiarotti, J. M. Sierchio, P. Bonoli, C. Kasten, D. A. Sutherland, H. S. Barnard, C. B. Haakonsen, J. Goh, C. Sung, and D. G. Whyte, "ARC: A compact, high-field, fusion nuclear science facility and demonstration power plant with demountable magnets," *Fusion Engineering and Design*, vol. 100, no. 2015, pp. 378-405.
- [3] A. Satoshi, W. Kazuo, O. Hidetoshi, M. Hiroshi, H. Satoshi, T. Taizo, and I. Shigeru, "First performance test of a 25 T cryogen-free superconducting magnet," *Superconductor Science and Technology*, vol. 30, no. 6, 2017, p. 065001.
- [4] Y. Sangwon, K. Jaemin, L. Hunju, H. Seungyong, and M. Seung-Hyun, "26 T 35 mm all-GdBa₂Cu₃O_{7-x} multi-width no-insulation superconducting magnet," *Superconductor Science and Technology*, vol. 29, no. 4, 2016, p. 04LT04.
- [5] H. Y. Bai, M. D. Bird, L. D. Cooley, I. R. Dixon, K. L. Kim, D. C. Larbalestier, W. S. Marshall, U. P. Trociewitz, H. W. Weijers, D. V. Abrahimov, and G. S. Boebinger, "The 40 T Superconducting Magnet Project at the National High Magnetic Field Laboratory," *Ieee Transactions on Applied Superconductivity*, vol. 30, no. 4, Jun 2020, p. 5.
- [6] D. Clazynski, "Review of Nb₃Sn conductors for ITER," *Fusion Engineering and Design*, vol. 82, no. 5-14, Oct 2007, pp. 488-497.
- [7] C. Senatore, M. Alessandrini, A. Lucarelli, R. Tediosi, D. Uglietti, and Y. Iwasa, "Progresses and challenges in the development of high-field solenoidal magnets based on RE₁₂₃ coated conductors," *Superconductor Science & Technology*, vol. 27, no. 10, Oct 2014, p. 26.
- [8] V. Solovyov and P. Farrell, "Exfoliated YBCO filaments for second-generation superconducting cable," *Superconductor Science and Technology*, vol. 30, no. 1, 2017, p. 014006.
- [9] J. D. Weiss, D. C. van der Laan, D. Hazelton, A. Knoll, G. Carota, D. Abrahimov, A. Francis, M. A. Small, G. Bradford, and J. Jaroszynski, "Introduction of the next generation of CORC (R) wires with engineering current density exceeding 650 A mm⁻² at 12T based on SuperPower's ReBCO tapes containing substrates of 25 μm thickness," *Superconductor Science & Technology*, vol. 33, no. 4, Apr 2020, p. 9.
- [10] M. Takayasu, L. Chiesa, L. Bromberg, and J. Minervini, V. , "HTS twisted stacked-tape cable conductor," *Superconductor Science and Technology*, vol. 25, no. 1, 2012, p. 014011.
- [11] V. Solovyov, S. Rabbani, M. Ma, Z. Mendleson, Z. Wang, A. Polyanskii, and P. Farrell, "Electromechanical Properties of 1-mm-Wide Superconducting Cables Comprised of Exfoliated YBCO Filaments," *IEEE Transactions on Applied Superconductivity*, vol. 29, no. 5, 2019, pp. 1-5.
- [12] G. Levin, P. Barnes, and J. Bulmer, "Current sharing between superconducting film and normal metal," *Superconductor Science and Technology*, vol. 20, no. 8, 2007, p. 757.
- [13] S. Yoon, K. Cheon, H. Lee, S.-H. Moon, S.-Y. Kim, Y. Kim, S.-H. Park, K. Choi, and G.-W. Hong, "The performance of the conduction cooled 2G HTS magnet wound without turn to turn insulation generating 4.1 T in 102 mm bore," *Physica C: Superconductivity*, vol. 494, no. 0, 2013, pp. 242-245.
- [14] Y. Li, "Analyzing full electromagnetic behaviors of no-insulation, high-temperature superconducting coils with turn-to-turn bypass currents and persistent screening currents," *Superconductor Science & Technology*, vol. 33, no. 8, Aug 2020, p. 3.